Supplementary Information

Non-Precious Macrocycle Embedded Hybrid Nanocomposites for Efficient Water Oxidation

Giddaerappa[a*], Sundarraj Sriram[a], P Abdul Junaid[a], Lokesh Koodlur Sannegowda[b], M.H. Naveen[c], K Sudhakara Prasad[a*]
[a] Nanomaterial Research Laboratory (NMRL), Smart Materials And Devices, Yenepoya (Deemed to be University), Deralakatte, Mangalore 575 018, India.
[b]Viajayanagara Sri Krishnadevaraya University, Ballari, Karnataka, india-583005
[c] Chemical Engineering Programm,Physcial Science and Engineering Division, King Abdullah University of Science and Technology (KAUST), Thuwal, 23955-6900, Saudi Arabia.
*Email: giddaerappa1234@gmail.com and ksprasadnair@yenepoya.edu.in

Content	Descriptions	Page

Chemicals and reagents

Analytical grade of tartaric acid ($C_4H_6O_6$), cobalt chloride hexahydrate ($CoCl_2.6H_2O$), 4-nitrophthalonitrile ($C_6H_4NO_2(CN)_2$), 1,8-diazabicyclo[5.4.0]undec-7-ene (DBU) ($C_9H_{16}N_2$), potassium carbonate (K_2CO_3), tetrabutylammonium perchlorate (TBAP) ($C_{16}H_{36}ClNO_4$), n-pentanol ($C_5H_{11}OH$), methanol (CH_3OH), ethanol (C_2H_5OH), acetone (CH_3COCH_3), n-hexane (C_6H_{14}), dimethylformamide (DMF) (C_3H_7NO), dimethylsulfoxide (DMSO) (C_2H_6OS), hydrochloric acid (HCl), potassium hydroxide (KOH), sulphuric acid (H_2SO_4), 20% Pt/C and IrO_2 were purchased from SD fine Chemicals or Sigma-Aldrich, India and used without further purification.

Physical methods

The melting point of the sample was determined using a melting point apparatus from Sisco instruments (Model no.70818209, India). The elemental analysis of the synthesized compounds was performed using a CHN&S elemental analyzer (Vario ELIII CHNS). The UV-Vis absorption spectrum of the sample was recorded in a quartz cuvette using an Ocean optics spectrometer with flame (FLAME-S-UV-VIS-ES, serial no. FLS04808) in the wavelength range 280-850 nm using 0.1 mM of Poly CoTAPc in DMSO. Fourier-transform infrared spectroscopy (FT-IR) analysis was performed using a Spectrum Two FT-IR spectrometer (Perkin Elmer) with a resolution of 1 cm^{-1} using KBr pellet method. The mass spectra (70 eV, electron impact mode) were measured using a Finnigan MAT instrument (Agilent). The thermal stability of the synthesized phthalocyanine was analyzed using a STA 6000 Simultaneous Thermal Analyzer (Perkin Elmer) in the temperature range of 30-700 °C at a heating rate of 20 $°C \cdot min^{-1}$ under air flow (30 $mL \cdot min^{-1}$). The X-ray diffraction (XRD) pattern of the sample was measured using a Bruker D8 Advance X-ray diffractometer. Transmission electron microscope (TEM) images were taken using a Talos F200S (ThermoFisher Scientific), and X-ray photoelectron spectroscopy (XPS) analysis were conducted using a SPECSMXPS system.

Calculation methods:

Mass activity: The mass activity (A g^{-1}) are measured from from the catalyst loading density m and the measured current density j(mA/cm^2) at η= 350 mV. The mass activity can be calculated by using the below formula [1].

$$\text{Mass activity}=j/m.$$

TOF: TOF is defined as the number of reactant that a catalyst can convert to a desired product per catalytic site per unit of time, exhibiting the intrinsic catalytic of each catalytic site [2]. The value of TOF is calculated by the following equation:

$$TOF=(jA)/(4Fn).$$

Here, j(mA.cm^{-2}) is the measured current density at a given potential (η= 350 mV), A is the surface area of the working electrode, 4 is the electron transfer number during O_2 generation, and n is the number of moles of the active materials. Assuming that all cobalt ions in the catalysts are active and contribute to the catalytic reaction (lowest TOF values were calculated), so n is the Co ions molar number calculated from catalysing loading amount, F is the Faraday constant (F = 96485 C mol^{-1}).

Roughness Factor (R_f): Roughness factor of the electrode is calculated by the following equation [3].

$$R_f = \text{ECSA/Electrode surface area}$$

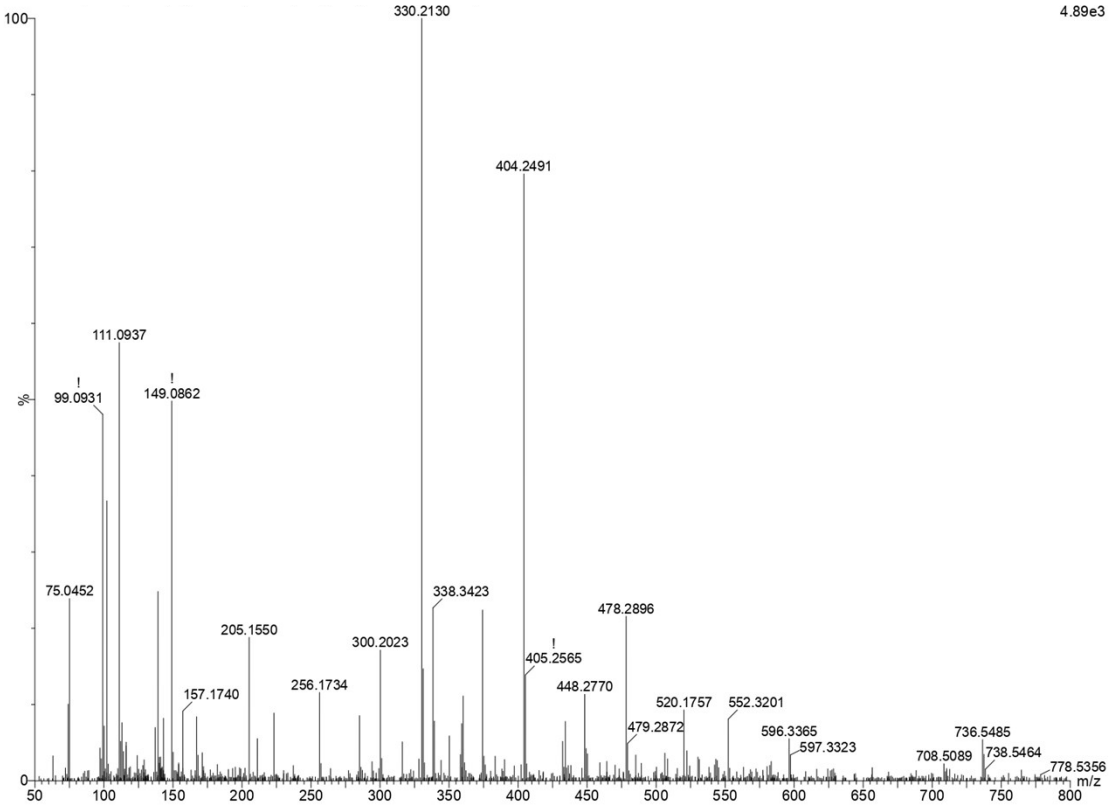

Figure S1. Mass spectrum of oxy-bridged ligand, ***3***.

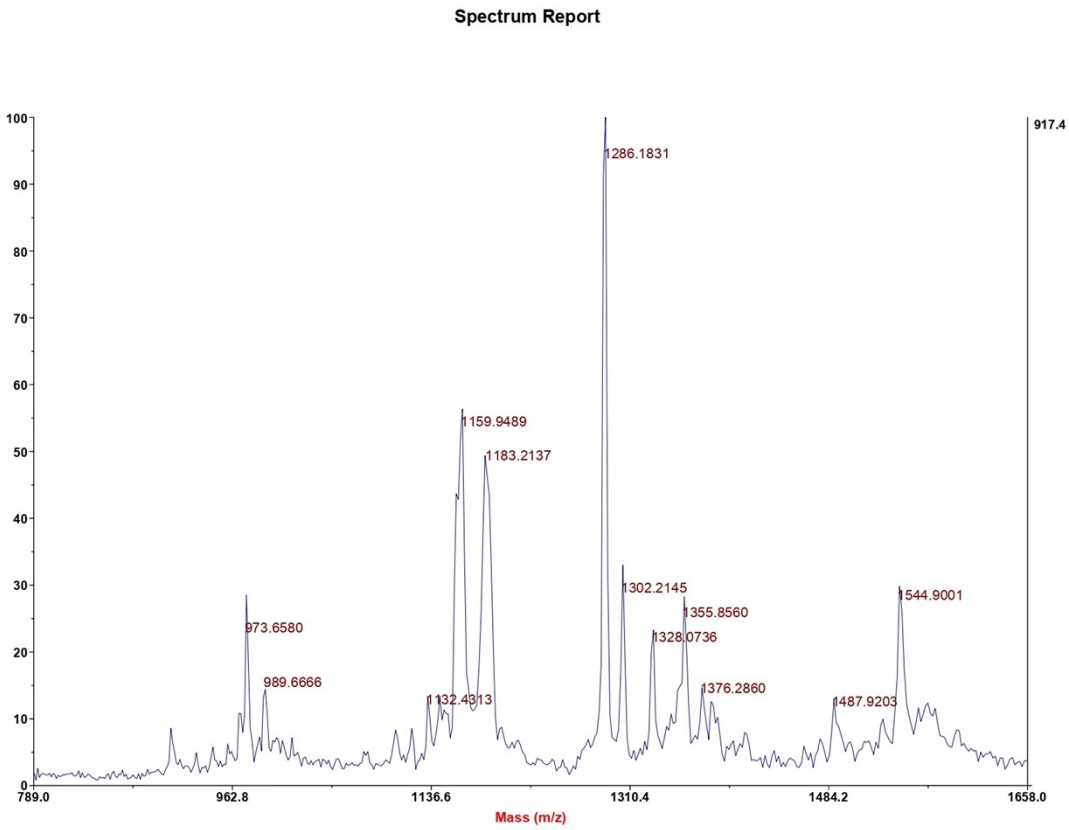

Figure S2. Mass spectrum of Poly CoTAPc.

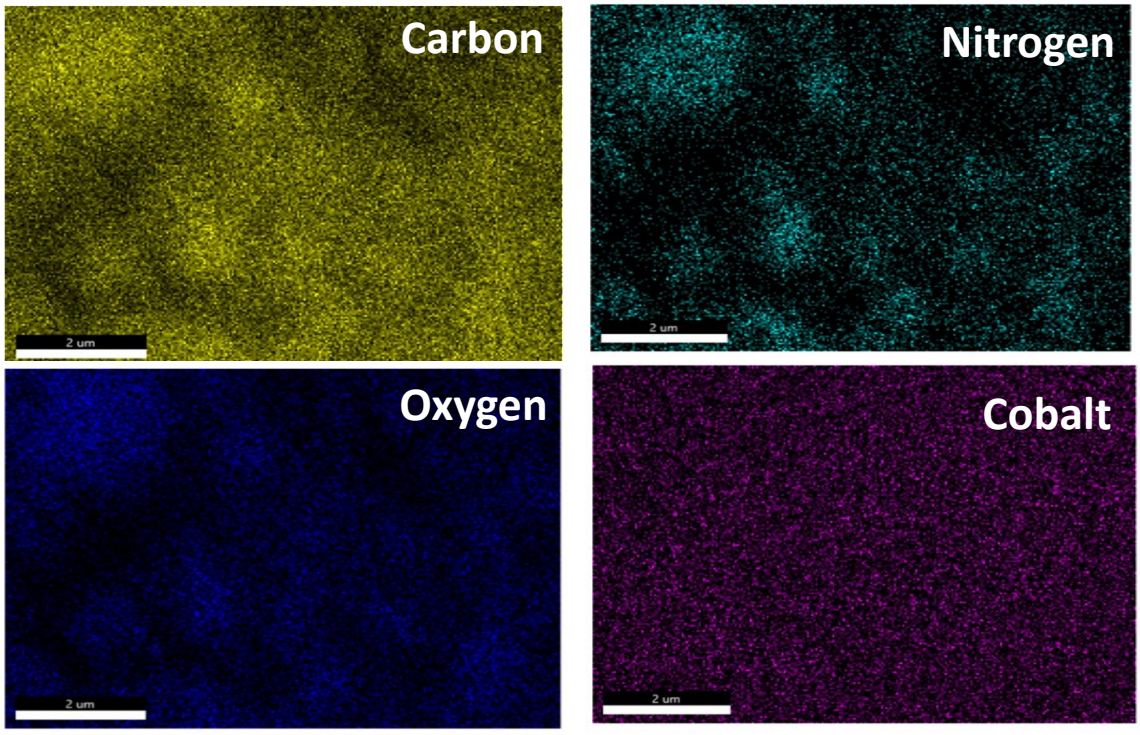

Figure S3. Elemental mapping of carbon, nitrogen, oxygen and cobalt in Poly CoTAPc.

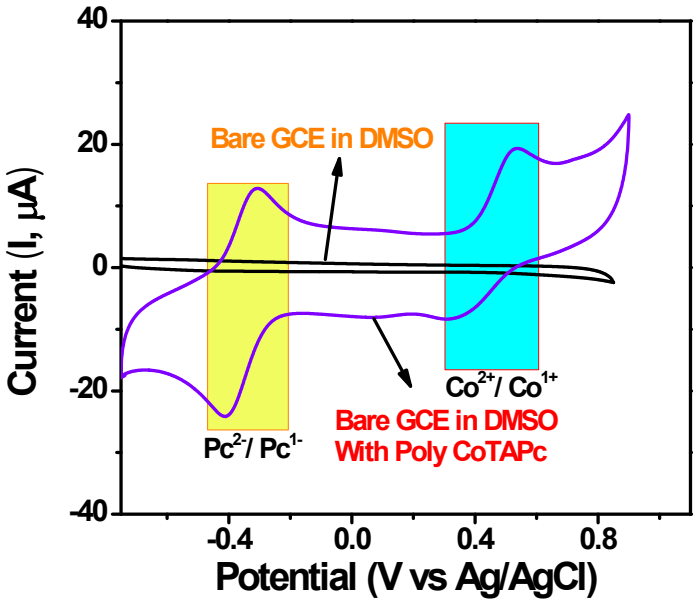

Figure S4. Solution CV response of Poly CoTAPc in DMSO electrolyte using GCE and TBAP as supporting electrolyte scanned at 50 $mV.s^{-1}$.

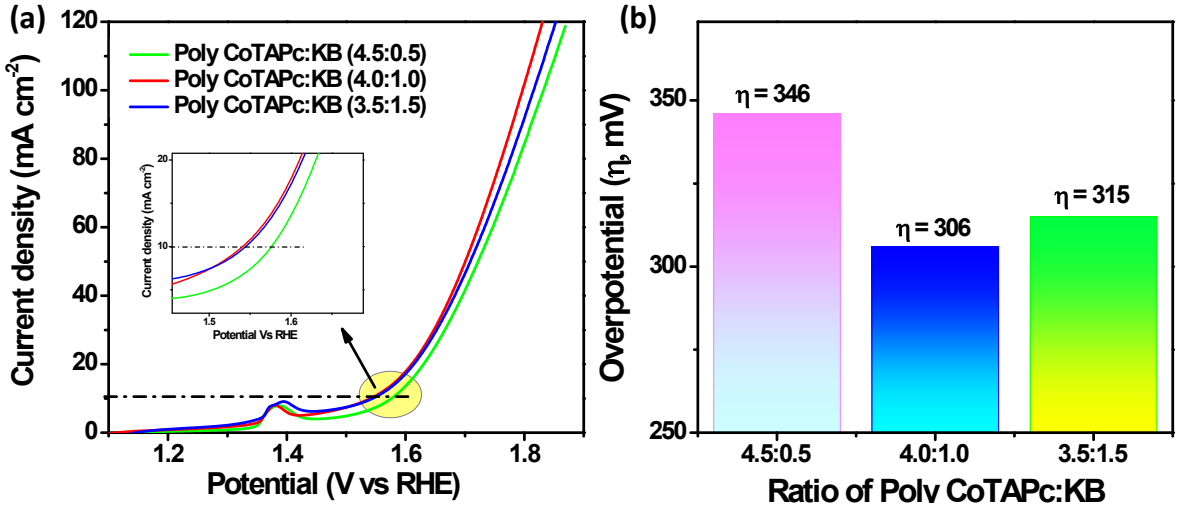

Figure S5. LSV polarization curves and overpotential bar graph of different composition of Poly CoTAPc:KB at 10 mA/cm^2.

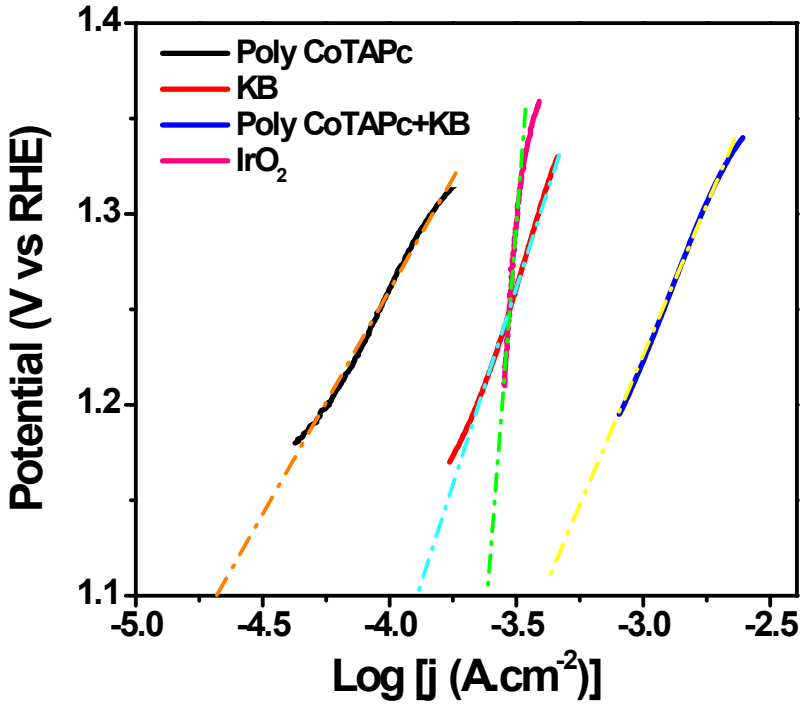

Figure S6. Estimated exchange current density of modified electrodes.

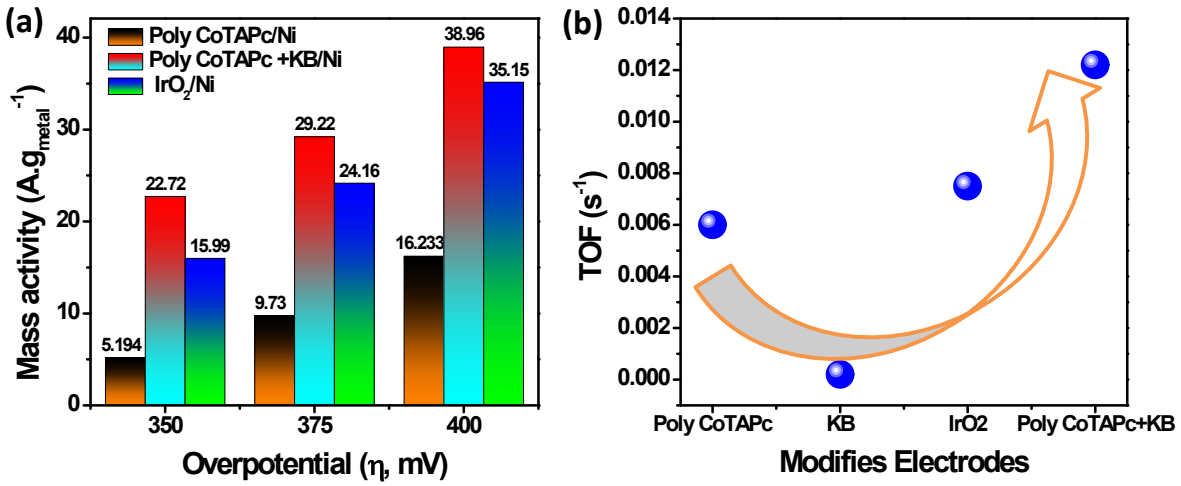

Figure S7. (a) Mass activity and (b) TOF value of catalysts modified electrode measured at a overpotential of 1.58V vs RHE.

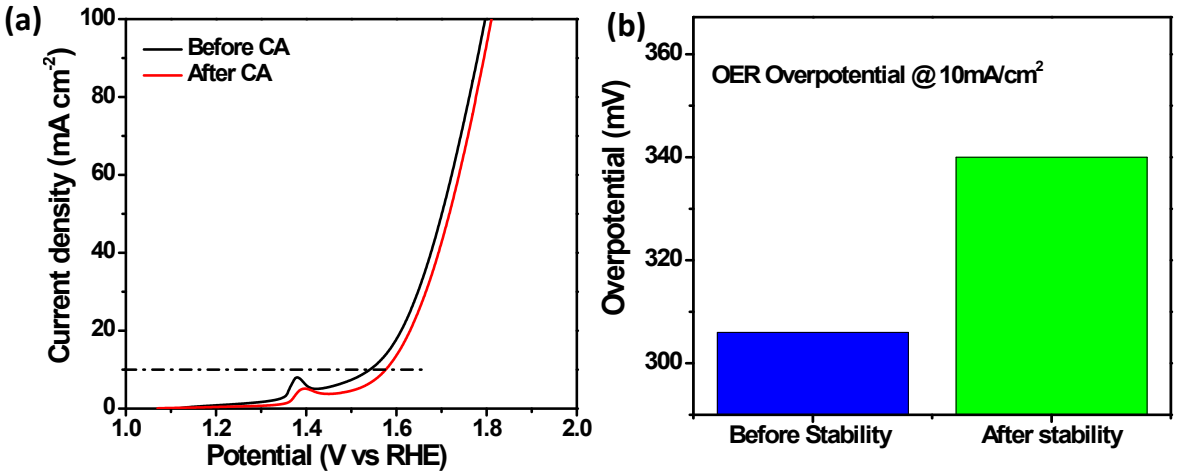

Figure S8. (a) LSV polarization curves for OER before and after chronoamperometric (CA) study carried with PolyCoTAPc+KB/Ni in 1M KOH with 5mV .cm^{-1} scan rate. (b) Overpotential needed to reach 10mA.cm-2 before and after chronoamperometric stability study.

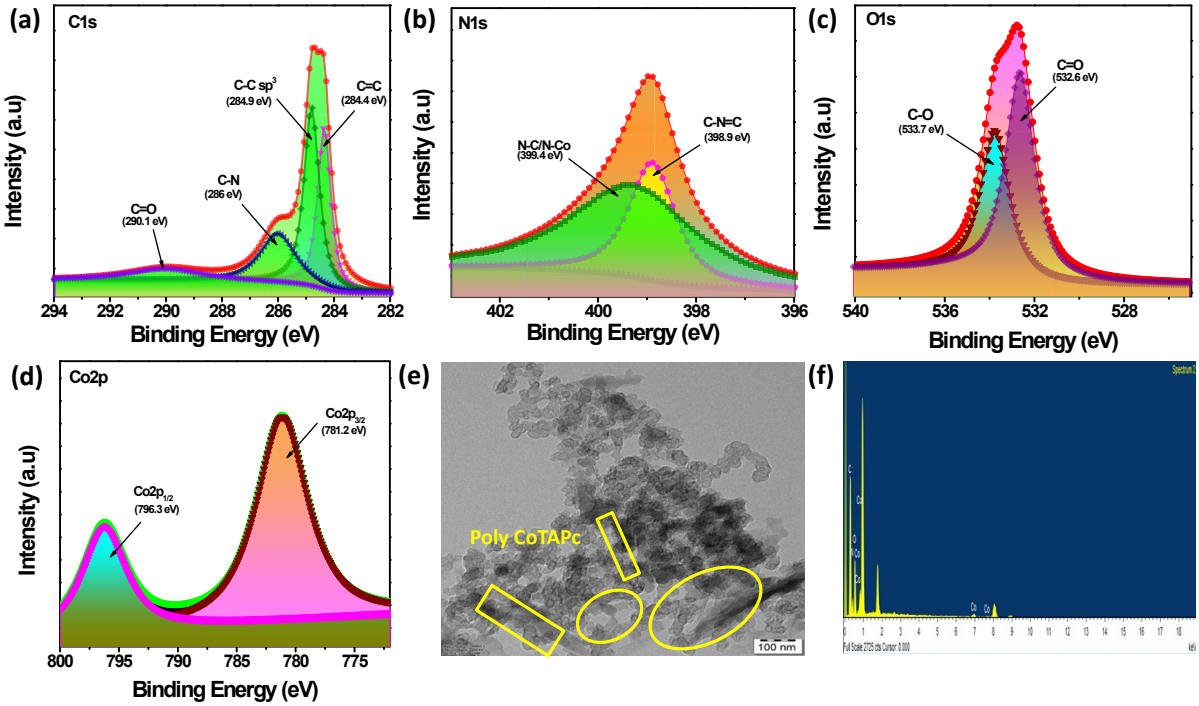

Figure S9. (a-d) XPS spectrum for each component, (e) HRTEM image and (f) EDAX image of hybrid composite Poly CoTAPc+KB after long term chronoamperometric stability test.

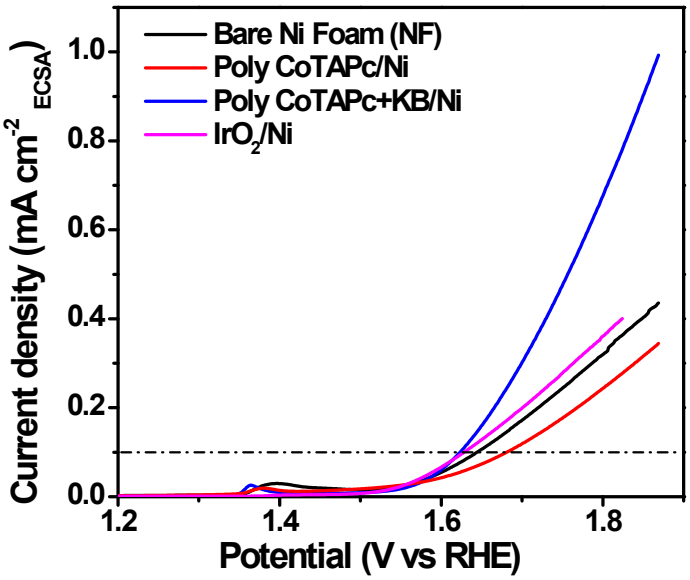

Figure S10. ECSA normalized LSV polarization curves of all fabricated electrode

Table S1. Comparison of OER activity of HQCoPc+KB with other non-noble electrocatalysts.

Catalysts	Electrolyte	Overpotential at 10 mA.cm^{-2}	Tafel slope (mV.dec^{-1})	References
Fe0.5Ni0.5Pc-CP	1 M KOH	317	116	4
FeNiN-MWCNT	0.1M KOH	350	-	5
Co@Co_3O_4	0.1 M KOH	420	125.3	6
Co/NCNT	1.0 M KOH	416	91	7
Poly [Co $^{(II)}$THTPc]: KB	1 M KOH	359	59.84	8
COOH defect graphene	1 M KOH	390	-	9
CoTTPc/MWCNTs	1 M KOH	305	63	10
α-MnO_2	1 M KOH	450	73.1	11
rGO-CoTATPc	1M KOH	373	45	12
NiCo LDH	1 M KOH	335	41	13
NiCoN NW	1.0 M NaOH	360	46.9	14
NiO/NC	1 M KOH	429	61.	15
Mn-Cd-S@Ni_3S_2	1 M KOH	333	150	16
Ni/FeOOH nanosheet	0.1 M KOH	390	78.3	17
PCN-CFP	0.1 M KOH	400	61.6	41
Poly CoTAPc+KB/Ni	**1 M KOH**	**306**	**81**	**Present work**

Table S2. EIS equivalent circuit parameters for fitting the Nyquist plots of different catalysts in 1M KOH.

Electrode	R_s(Ω) (% RSD)	Q-Yo (% RSD)	Q-n (% RSD)	R_c(Ω) (% RSD)	Q-Yo (% RSD)	Q-n (% RSD)	R_{ct} (Ω) (% RSD)
Ni foam	3.45 (8.29)	0.013 (117.6)	0.8 (35.25)	2.619 (48.47)	0.002 (2.89)	0.85 (1.749)	27 (3.58)
PolyCoTAPc	3.509 (0.9234)	0.005601 (63.56)	0.8792 (8.896)	0.4791 (10.34)	0.004317 (1.373)	0.8222 (0.464)	24.41 (0.5199)
KB	3.507 (0.9892)	0.07932 (58.32)	0.8 (8.748)	0.5364 (9.897)	0.004182 (1.277)	0.8 (0.436)	25.69 (0.4969)
PolyCoTAPc+KB	3.465 (1.54)	0.0017 (85.95)	0.75 (14.45)	0.6 (16.26)	0.0040 (2.151)	0.837 (0.77)	20.05 (0.7928)

Reference

1. Zhang, H., Zheng, J., Chao, Y., Zhang, K., & Zhu, Z. (2018). Surface engineering of FeCo-based electrocatalysts supported on carbon paper by incorporating non-noble metals for water oxidation. *New Journal of Chemistry*, *42*(9), 7254–7261. https://doi.org/10.1039/C7NJ04941B
2. Sriram, S., Vishnu, B., & Jayabharathi, J. (2023). Ultrathin cobalt phosphate enfolded with biomass-derived multishelled carbon onion as a proficient electrocatalyst for the oxygen evolution reaction and its green sustainability assessments. *New Journal of Chemistry*, *47*(41), 19210–19222. https://doi.org/10.1039/D3NJ03346E
3. Sriram, S., Vishnu, B., & Jayabharathi, J. (2023). Solution combusted ultrathin Co_3O_4/CoO heterophase electrocatalyst for solar-energy driven bifunctional water electrolysis. *ChemistrySelect*, *8*(30). https://doi.org/10.1002/slct.202301402
4. Qi, D., Chen, X., Liu, W., Liu, C., Liu, W., Wang, K., & Jiang, J. (2020). A Ni/Fe-based heterometallic phthalocyanine conjugated polymer for the oxygen evolution reaction. *Inorganic Chemistry Frontiers*, *7*(3), 642–646. https://doi.org/10.1039/C9QI01325C
5. Kumar, Y., Kibena-Põldsepp, E., Kozlova, J., Rähn, M., Treshchalov, A., Kikas, A., Kisand, V., Aruväli, J., Tamm, A., Douglin, J. C., Folkman, S. J., Gelmetti, I., Garcés-Pineda, F. A., Galán-Mascarós, J. R., Dekel, D. R., & Tammeveski, K. (2021). Bifunctional Oxygen Electrocatalysis on Mixed Metal Phthalocyanine-Modified Carbon Nanotubes Prepared via Pyrolysis. *ACS Applied Materials & Interfaces*, *13*(35), 41507–41516. https://doi.org/10.1021/acsami.1c06737
6. Aijaz, A., Masa, J., Rösler, C., Xia, W., Weide, P., Botz, A. J. R., Fischer, R. A., Schuhmann, W., & Muhler, M. (2016). Co@Co_3O_4 Encapsulated in Carbon Nanotube-Grafted Nitrogen-Doped Carbon Polyhedra as an Advanced Bifunctional Oxygen Electrode. *Angewandte Chemie International Edition*, *55*(12), 4087–4091. https://doi.org/10.1002/anie.201509382
7. Das, D., Das, A., Reghunath, M., & Nanda, K. K. (2017). Phosphine-free avenue to Co_2P nanoparticle encapsulated N,P co-doped CNTs: a novel non-enzymatic glucose sensor and an efficient electrocatalyst for oxygen evolution reaction. *Green Chemistry*, *19*(5), 1327–1335. https://doi.org/10.1039/C7GC00084G
8. Kousar, N., Thimmappa, R., Giddaerappa, Palanna, M., & Sannegowda, L. K. (2024). Phthalocyanine Polymer Anchored Ketjen Black Nanoparticles for Bifunctional

Oxygen Electrocatalysis. *ACS Applied Nano Materials*, *7*(9), 10600–10613. https://doi.org/10.1021/acsanm.4c01044

9. Liu, Z., Zhao, Z., Wang, Y., Dou, S., Yan, D., Liu, D., Xia, Z., & Wang, S. (2017). In Situ Exfoliated, Edge-Rich, Oxygen-Functionalized Graphene from Carbon Fibers for Oxygen Electrocatalysis. *Advanced Materials*, *29*(18). https://doi.org/10.1002/adma.201606207
10. Kumbara, A. C., Kousar, N., Giddaerappa, & Sannegowda, L. K. (2024). Bioinspired cobalt phthalocyanine hybrid as bifunctional electrocatalyst for oxygen electrocatalysis. *Journal of Energy Storage*, *97*, 112920. https://doi.org/10.1016/j.est.2024.112920
11. Han, G.-Q., Liu, Y.-R., Hu, W.-H., Dong, B., Li, X., Shang, X., Chai, Y.-M., Liu, Y.-Q., & Liu, C.-G. (2016). Crystallographic Structure and Morphology Transformation of MnO_2 Nanorods as Efficient Electrocatalysts for Oxygen Evolution Reaction. *Journal of The Electrochemical Society*, *163*(2), H67–H73. https://doi.org/10.1149/2.0371602jes
12. Chandrakala, K. B., Giddaerappa, Venugopala Reddy, K. R., & Shivaprasad, K. H. (2022). Investigational undertaking descriptors for reduced graphene oxide-phthalocyanine composite based catalyst for electrochemical oxygen evolution reaction. *Journal of Electroanalytical Chemistry*, *919*, 116558. https://doi.org/10.1016/j.jelechem.2022.116558
13. Song, F., & Hu, X. (2014). Exfoliation of layered double hydroxides for enhanced oxygen evolution catalysis. *Nature Communications*, *5*(1), 4477. https://doi.org/10.1038/ncomms5477
14. Han, L., Feng, K., & Chen, Z. (2017). Self-Supported Cobalt Nickel Nitride Nanowires Electrode for Overall Electrochemical Water Splitting. *Energy Technology*, *5*(11), 1908–1911. https://doi.org/10.1002/ente.201700108
15. Seok, S., Jang, D., Kim, H., & Park, S. (2020). Production of NiO/N-doped carbon hybrid and its electrocatalytic performance for oxygen evolution reactions. *Carbon Letters*, *30*(5), 485–491. https://doi.org/10.1007/s42823-019-00118-9
16. Li, Z., Wang, X., Wang, X., Lin, Y., Meng, A., Yang, L., & Li, Q. (2019). Mn-Cd-S@amorphous-Ni3S2 hybrid catalyst with enhanced photocatalytic property for hydrogen production and electrocatalytic OER. *Applied Surface Science*, *491*, 799–806. https://doi.org/10.1016/j.apsusc.2019.05.313

17. Lee, J., Lee, H., & Lim, B. (2018). Chemical transformation of iron alkoxide nanosheets to FeOOH nanoparticles for highly active and stable oxygen evolution electrocatalysts. *Journal of Industrial and Engineering Chemistry*, *58*, 100–104. https://doi.org/10.1016/j.jiec.2017.09.013
18. Ma, T. Y., Ran, J., Dai, S., Jaroniec, M., & Qiao, S. Z. (2015). Phosphorus-Doped Graphitic Carbon Nitrides Grown In Situ on Carbon-Fiber Paper: Flexible and Reversible Oxygen Electrodes. *Angewandte Chemie International Edition*, *54*(15), 4646–4650. https://doi.org/10.1002/anie.201411125